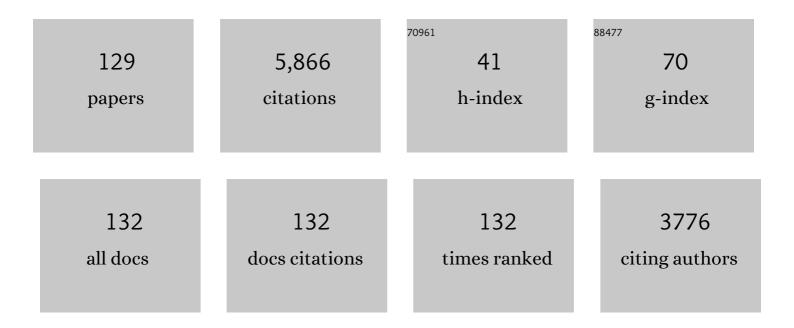
List of Publications by Year in descending order

Source: https://exaly.com/author-pdf/2045255/publications.pdf Version: 2024-02-01



Комстнаци

#	Article	IF	CITATIONS
1	Designed oxygen carriers from macroporous LaFeO3 supported CeO2 for chemical-looping reforming of methane. Applied Catalysis B: Environmental, 2017, 202, 51-63.	10.8	306
2	Exploring the ternary interactions in Cu–ZnO–ZrO2 catalysts for efficient CO2 hydrogenation to methanol. Nature Communications, 2019, 10, 1166.	5.8	258
3	CO ₂ Hydrogenation to Methanol over ZrO ₂ -Containing Catalysts: Insights into ZrO ₂ Induced Synergy. ACS Catalysis, 2019, 9, 7840-7861.	5.5	253
4	Ce–Fe oxygen carriers for chemical-looping steam methane reforming. International Journal of Hydrogen Energy, 2013, 38, 4492-4501.	3.8	191
5	Syngas production from methane and air via a redox process using Ce–Fe mixed oxides as oxygen carriers. Applied Catalysis B: Environmental, 2010, 97, 361-372.	10.8	183
6	Perovskites as Geo-inspired Oxygen Storage Materials for Chemical Looping and Three-Way Catalysis: A Perspective. ACS Catalysis, 2018, 8, 8213-8236.	5.5	152
7	Structure dependence and reaction mechanism of CO oxidation: A model study on macroporous CeO2 and CeO2-ZrO2 catalysts. Journal of Catalysis, 2016, 344, 365-377.	3.1	148
8	Chemical-Looping Steam Methane Reforming over a CeO ₂ –Fe ₂ O ₃ Oxygen Carrier: Evolution of Its Structure and Reducibility. Energy & Fuels, 2014, 28, 754-760.	2.5	137
9	Strong Evidence of the Role of H2O in Affecting Methanol Selectivity from CO2 Hydrogenation over Cu-ZnO-ZrO2. CheM, 2020, 6, 419-430.	5.8	130
10	Direct conversion of methane to synthesis gas using lattice oxygen of CeO2–Fe2O3 complex oxides. Chemical Engineering Journal, 2010, 156, 512-518.	6.6	125
11	Transformation of methane into synthesis gas using the redox property of Ce–Fe mixed oxides: Effect of calcination temperature. International Journal of Hydrogen Energy, 2011, 36, 3471-3482.	3.8	118
12	Density functional theory studies of transition metal carbides and nitrides as electrocatalysts. Chemical Society Reviews, 2021, 50, 12338-12376.	18.7	103
13	Confined Ni-In intermetallic alloy nanocatalyst with excellent coking resistance for methane dry reforming. Journal of Energy Chemistry, 2022, 65, 34-47.	7.1	96
14	Chemical Looping Conversion of Gaseous and Liquid Fuels for Chemical Production: A Review. Energy & Fuels, 2020, 34, 5381-5413.	2.5	95
15	Chemical looping reforming of methane using magnetite as oxygen carrier: Structure evolution and reduction kinetics. Applied Energy, 2018, 211, 1-14.	5.1	93
16	Chemical‣ooping Conversion of Methane: A Review. Energy Technology, 2020, 8, 1900925.	1.8	87
17	Removal and immobilization of arsenic from copper smelting wastewater using copper slag by in situ encapsulation with silica gel. Chemical Engineering Journal, 2020, 394, 124833.	6.6	86
18	Partial oxidation of methane to syngas with air by lattice oxygen transfer over ZrO2-modified Ce–Fe mixed oxides. Chemical Engineering Journal, 2011, 173, 574-582.	6.6	83

#	Article	IF	CITATIONS
19	Hydrogen and syngas production from two-step steam reforming of methane over CeO2-Fe2O3 oxygen carrier. Journal of Rare Earths, 2010, 28, 907-913.	2.5	81
20	Soot combustion over Ce1-xFexO2-Î′ and CeO2/Fe2O3 catalysts: Roles of solid solution and interfacial interactions in the mixed oxides. Applied Surface Science, 2016, 390, 513-525.	3.1	80
21	Synergy effects of combined red muds as oxygen carriers for chemical looping combustion of methane. Chemical Engineering Journal, 2018, 341, 588-600.	6.6	73
22	Enhanced reducibility and redox stability of Fe ₂ O ₃ in the presence of CeO ₂ nanoparticles. RSC Advances, 2014, 4, 47191-47199.	1.7	70
23	Ceria-nano supported copper oxide catalysts for CO preferential oxidation: Importance of oxygen species and metal-support interaction. Applied Surface Science, 2019, 494, 1166-1176.	3.1	69
24	DFT insights into oxygen vacancy formation and CH ₄ activation over CeO ₂ surfaces modified by transition metals (Fe, Co and Ni). Physical Chemistry Chemical Physics, 2018, 20, 11912-11929.	1.3	64
25	Enhanced CH ₄ and CO Oxidation over Ce _{1–<i>x</i>} Fe <i>_x</i> O _{2â[^]î} Hybrid Catalysts by Tuning the Lattice Distortion and the State of Surface Iron Species. ACS Applied Materials & amp; Interfaces, 2019, 11, 19227-19241.	4.0	64
26	Structure dependence of Nb2O5-X supported manganese oxide for catalytic oxidation of propane: Enhanced oxidation activity for MnOx on a low surface area Nb2O5-X. Applied Catalysis B: Environmental, 2019, 244, 438-447.	10.8	64
27	Preparation and characterization of Ce1-Fe O2 complex oxides and its catalytic activity for methane selective oxidation. Journal of Rare Earths, 2008, 26, 245-249.	2.5	61
28	Chemical-looping steam methane reforming over macroporous CeO2–ZrO2 solid solution: Effect of calcination temperature. International Journal of Hydrogen Energy, 2014, 39, 13361-13368.	3.8	61
29	Interfacial Active Sites for CO2 Assisted Selective Cleavage of C–C/C–H Bonds in Ethane. CheM, 2020, 6, 2703-2716.	5.8	57
30	Chemical-looping water splitting over ceria-modified iron oxide: Performance evolution and element migration during redox cycling. Chemical Engineering Science, 2018, 179, 92-103.	1.9	56
31	Ce1-xFexO2-δ catalysts for catalytic methane combustion: Role of oxygen vacancy and structural dependence. Catalysis Today, 2018, 318, 73-85.	2.2	55
32	Ce-Fe-O mixed oxide as oxygen carrier for the direct partial oxidation of methane to syngas. Journal of Rare Earths, 2010, 28, 560-565.	2.5	52
33	A yolk/shell strategy for designing hybrid phase change materials for heat management in catalytic reactions. Journal of Materials Chemistry A, 2017, 5, 24232-24246.	5.2	52
34	Efficient removal of arsenic from copper smelting wastewater in form of scorodite using copper slag. Journal of Cleaner Production, 2020, 270, 122428.	4.6	51
35	CeO2 modified Fe2O3 for the chemical hydrogen storage and production via cyclic water splitting. International Journal of Hydrogen Energy, 2014, 39, 13381-13388.	3.8	50
36	Hydrogen and syngas production from two-step steam reforming of methane using CeO2 as oxygen carrier. Journal of Natural Gas Chemistry, 2011, 20, 281-286.	1.8	48

#	Article	IF	CITATIONS
37	Bulk monolithic Ce–Zr–Fe–O/Al 2 O 3 oxygen carriers for a fixed bed scheme of the chemical looping combustion: Reactivity of oxygen carrier. Applied Energy, 2016, 163, 19-31.	5.1	47
38	Enhanced performance of red mud-based oxygen carriers by CuO for chemical looping combustion of methane. Applied Energy, 2019, 253, 113534.	5.1	46
39	Self-enhanced and efficient removal of arsenic from waste acid using magnetite as an in situ iron donator. Water Research, 2019, 157, 269-280.	5.3	46
40	Modification of CeO2 on the redox property of Fe2O3. Materials Letters, 2013, 93, 129-132.	1.3	45
41	Enhanced Activity of CeO ₂ –ZrO ₂ Solid Solutions for Chemical-Looping Reforming of Methane via Tuning the Macroporous Structure. Energy & Fuels, 2016, 30, 638-647.	2.5	44
42	Catalytic performance of cerium iron complex oxides for partial oxidation of methane to synthesis gas. Journal of Rare Earths, 2008, 26, 705-710.	2.5	42
43	Effects of Co3O4 nanocatalyst morphology on CO oxidation: Synthesis process map and catalytic activity. Chinese Journal of Catalysis, 2016, 37, 908-922.	6.9	41
44	Effects of rare-earth (Nd, Er and Y) doping on catalytic performance of HZSM-5 zeolite catalysts for methyl mercaptan (CH3SH) decomposition. Applied Catalysis A: General, 2017, 533, 66-74.	2.2	41
45	Enhanced activity and stability of Sm-doped HZSM-5 zeolite catalysts for catalytic methyl mercaptan (CH 3 SH) decomposition. Chemical Engineering Journal, 2017, 317, 60-69.	6.6	41
46	Effect of transition metal Fe adsorption on CeO 2 (110) surface in the methane activation and oxygen vacancy formation: A density functional theory study. Applied Surface Science, 2017, 416, 547-564.	3.1	41
47	A quantitative study on the interaction between curvature and buoyancy effects in helically coiled heat exchangers of supercritical CO2 Rankine cycles. Energy, 2016, 116, 661-676.	4.5	39
48	Performance of cubic ZrO2 doped CeO2: First-principles investigation on elastic, electronic and optical properties of Ce1â^ Zr O2. Journal of Alloys and Compounds, 2016, 671, 208-219.	2.8	39
49	Enhanced performance of copper ore oxygen carrier by red mud modification for chemical looping combustion. Applied Energy, 2020, 277, 115590.	5.1	39
50	Ce-Fe-Zr-O/MgO coated monolithic oxygen carriers for chemical looping reforming of methane to co-produce syngas and H2. Chemical Engineering Journal, 2020, 388, 124190.	6.6	39
51	Preparation and characterization of Ce1-x NixO2 as oxygen carrier for selective oxidation methane to syngas in absence of gaseous oxygen. Journal of Rare Earths, 2010, 28, 357-361.	2.5	37
52	Microstructure and oxygen evolution of Fe–Ce mixed oxides by redox treatment. Applied Surface Science, 2014, 289, 378-383.	3.1	37
53	Chemical Looping Co-splitting of H ₂ O–CO ₂ for Efficient Generation of Syngas. ACS Sustainable Chemistry and Engineering, 2019, 7, 15452-15462.	3.2	37
54	Stochastic ecological kinetics of regime shifts in a timeâ€delayed lake eutrophication ecosystem. Ecosphere, 2017, 8, e01805.	1.0	36

#	Article	IF	CITATIONS
55	Synergy of red mud oxygen carrier with MgO and NiO for enhanced chemical-looping combustion. Energy, 2020, 197, 117202.	4.5	36
56	Evaluation of Fe substitution in perovskite LaMnO3 for the production of high purity syngas and hydrogen. Journal of Power Sources, 2020, 449, 227505.	4.0	35
57	oxides: <mml:math <br="" altimg="si0010.gif" xmlns:mml="http://www.w<sup>3</sup>.org/1998/Math/MathML">overflow="scroll"><mml:msub><mml:mrow><mml:mi>Ce</mml:mi></mml:mrow><mml:mrow><mml:mrow><mml:mrow>mathvariant="normal">M</mml:mrow><mml:mrow><mml:mn>0.25</mml:mn>mathvariant="normal">O</mml:mrow><mml:mrow><mm. 2016.<="" communications,="" solid="" state="" td=""><td>5hl:msub><m< td=""><td>>ml:msub><m< td=""></m<></td></m<></td></mm.></mml:mrow></mml:mrow></mml:mrow></mml:msub></mml:math>	5hl:msub> <m< td=""><td>>ml:msub><m< td=""></m<></td></m<>	>ml:msub> <m< td=""></m<>
58	Automatical and a second se	1.5	33
59	Syngas production modified by oxygen vacancies over CeO2-ZrO2-CuO oxygen carrier via chemical looping reforming of methane. Applied Surface Science, 2019, 481, 151-160.	3.1	32
60	Disposal of high-arsenic waste acid by the stepwise formation of gypsum and scorodite. RSC Advances, 2020, 10, 29-42.	1.7	32
61	Highly efficient reduction of O2-containing CO2 via chemical looping based on perovskite nanocomposites. Nano Energy, 2020, 78, 105320.	8.2	32
62	Hydrogen generation from water splitting over polyfunctional perovskite oxygen carriers by using coke oven gas as reducing agent. Applied Catalysis B: Environmental, 2022, 301, 120778.	10.8	32
63	CO Oxidation on Au/α-Fe ₂ O ₃ -Hollow Catalysts: General Synthesis and Structural Dependence. Journal of Physical Chemistry C, 2017, 121, 12696-12710.	1.5	31
64	Optimized Ni-based catalysts for methane reforming with O2-containing CO2. Applied Catalysis B: Environmental, 2021, 289, 120033.	10.8	31
65	Characteristic of macroporous CeO2-ZrO2 oxygen carrier for chemical-looping steam methane reforming. Journal of Rare Earths, 2014, 32, 842-848.	2.5	30
66	Chemical looping combustion of methane in a large laboratory unit: Model study on the reactivity and effective utilization of typical oxygen carriers. Chemical Engineering Journal, 2017, 328, 382-396.	6.6	30
67	Facile Synthesis of Al@Al ₂ O ₃ Microcapsule for High-Temperature Thermal Energy Storage. ACS Sustainable Chemistry and Engineering, 2018, 6, 13226-13236.	3.2	30
68	Hydrogen production via chemical looping reforming of coke oven gas. Green Energy and Environment, 2021, 6, 678-692.	4.7	30
69	Chemical interaction of Ce-Fe mixed oxides for methane selective oxidation. Journal of Rare Earths, 2014, 32, 824-830.	2.5	29
70	Optimization of Ni-Based Catalysts for Dry Reforming of Methane via Alloy Design: A Review. Energy & Fuels, 2022, 36, 5102-5151.	2.5	29
71	Limonite as a source of solid iron in the crystallization of scorodite aiming at arsenic removal from smelting wastewater. Journal of Cleaner Production, 2021, 278, 123552.	4.6	28
72	Reaction characteristics of chemical-looping steam methane reforming over a Ce–ZrO2 solid solution oxygen carrier. Mendeleev Communications, 2011, 21, 221-223.	0.6	27

#	Article	IF	CITATIONS
73	Enhanced activity of La1-xMnCuxO3 perovskite oxides for chemical looping steam methane reforming. Fuel Processing Technology, 2021, 215, 106744.	3.7	27
74	Enhanced propane and carbon monoxide oxidation activity by structural interactions of CeO2 with MnOx/Nb2O5-x catalysts. Applied Catalysis B: Environmental, 2020, 267, 118363.	10.8	26
75	Improved activity of magnetite oxygen carrier for chemical looping steam reforming by ultrasonic treatment. Applied Energy, 2020, 261, 114437.	5.1	26
76	Design of hybrid oxygen carriers with CeO2 particles on MnCo2O4 microspheres for chemical looping combustion. Chemical Engineering Journal, 2021, 404, 126554.	6.6	25
77	Self-generated Ni nanoparticles/LaFeO3 heterogeneous oxygen carrier for robust CO2 utilization under a cyclic redox scheme. Nano Energy, 2021, 89, 106379.	8.2	25
78	Ultra-Fine CeO ₂ Particles Triggered Strong Interaction with LaFeO ₃ Framework for Total and Preferential CO Oxidation. ACS Applied Materials & Interfaces, 2020, 12, 42274-42284.	4.0	24
79	Orientation effect in helical coils with smooth and rib-roughened wall: Toward improved gas heaters for supercritical carbon dioxide Rankine cycles. Energy, 2017, 140, 530-545.	4.5	23
80	NiO and CuO coated monolithic oxygen carriers for chemical looping combustion of methane. Journal of the Energy Institute, 2021, 94, 199-209.	2.7	23
81	Synthesis, CO2-tolerance and rate-determining step of Nb-doped Ce0.8Gd0.2O2â^îî–Pr0.6Sr0.4Co0.5Fe0.5O3â~îî ceramic membranes. Ceramics International, 2017, 43, 6477-6486.	2.3	22
82	Enhanced performance of chemical looping combustion of methane by combining oxygen carriers via optimizing the stacking sequences. Applied Energy, 2018, 230, 696-711.	5.1	22
83	Enhanced performance of LaFeO3 oxygen carriers by NiO for chemical looping partial oxidation of methane. Fuel Processing Technology, 2022, 236, 107396.	3.7	22
84	Structure and catalytic property of CeO2-ZrO2-Fe2O3 mixed oxide catalysts for diesel soot combustion: Effect of preparation method. Journal of Rare Earths, 2014, 32, 817-823.	2.5	21
85	The mechanism of photocatalyst and the effects of co-doping CeO2 on refractive index and reflectivity from DFT calculation. Computational Materials Science, 2019, 158, 197-208.	1.4	21
86	Syngas production from methane over CeO2-Fe2O3 mixed oxides using a chemical-looping method. Kinetics and Catalysis, 2013, 54, 326-333.	0.3	20
87	Iron-rich copper ore as a promising oxygen carrier for chemical looping combustion of methane. Journal of the Taiwan Institute of Chemical Engineers, 2019, 101, 204-213.	2.7	20
88	Enhanced resistance to carbon deposition in chemical-looping combustion of methane: Synergistic effect of different oxygen carriers via sequence filling. Chemical Engineering Journal, 2021, 421, 129776.	6.6	20
89	Bifunctional Mn-Cu-CeOx/γ-Al2O3 catalysts for low-temperature simultaneous removal of NOx and CO. Fuel, 2022, 321, 124050.	3.4	20
90	Pyrolysis of arsenic-bearing gypsum sludge being substituted for calcium flux in smelting process. Journal of Analytical and Applied Pyrolysis, 2018, 130, 19-28.	2.6	19

#	Article	IF	CITATIONS
91	Moderate-temperature chemical looping splitting of CO2 and H2O for syngas generation. Chemical Engineering Journal, 2020, 397, 125393.	6.6	19
92	Encapsulated Co3O4/(SiAl@Al2O3) thermal storage functional catalysts for catalytic combustion of lean methane. Applied Thermal Engineering, 2020, 181, 116012.	3.0	18
93	Chemical-looping reforming of methane over La-Mn-Fe-O oxygen carriers: Effect of calcination temperature. Chemical Engineering Science, 2021, 229, 116085.	1.9	18
94	Modified Al@Al2O3 phase change materials by carbon via in-situ catalytic decomposition of methane. Solar Energy Materials and Solar Cells, 2019, 200, 109924.	3.0	17
95	Separation of As from high As-Sb dust using Fe2O3 as a fixative under O2-N2 atmosphere. Separation and Purification Technology, 2018, 194, 81-88.	3.9	17
96	Suppressing byproduct formation for high selective CO2 reduction over optimized Ni/TiO2 based catalysts. Journal of Energy Chemistry, 2022, 72, 465-478.	7.1	17
97	Synthesis of mesoporous PrxZr1â^'xO2â [~] î^ solid solution with high thermal stability for catalytic soot oxidation. Journal of Industrial and Engineering Chemistry, 2017, 54, 126-136.	2.9	16
98	Modification of KNO ₃ on the reducibility and reactivity of Fe ₂ O ₃ â€based oxygen carriers for chemicalâ€looping combustion of methane. Canadian Journal of Chemical Engineering, 2017, 95, 1569-1578.	0.9	15
99	Enhanced performance of red mud for chemical-looping combustion of coal by the modification of transition metal oxides. Journal of the Energy Institute, 2022, 102, 22-31.	2.7	15
100	Preparation and characterization of Ce-Fe-Zr-O(x)/MgO complex oxides for selective oxidation of methane to synthesize gas. Journal of Rare Earths, 2010, 28, 316-321.	2.5	14
101	Enhanced Performance of Chemical Looping Combustion of CO with CaSO ₄ -CaO Oxygen Carrier. Energy & Fuels, 2017, 31, 5255-5265.	2.5	14
102	Phase transformation of Sn in tin-bearing iron concentrates by roasting with FeS2 in CO-CO2 mixed gases and its effects on Sn separation. Journal of Alloys and Compounds, 2018, 750, 8-16.	2.8	13
103	Catalytic combustion of lean methane over MnCo2O4/SiC catalysts: Enhanced activity and sulfur resistance. Fuel, 2022, 323, 124399.	3.4	13
104	Characteristics of CaS–CaO Oxidation for Chemical Looping Combustion with a CaSO ₄ -Based Oxygen Carrier. Energy & Fuels, 2017, 31, 13842-13851.	2.5	12
105	Sn separation from Sn-bearing iron concentrates by roasting with waste tire rubber in N2 + CO +â mixed gases. Journal of Hazardous Materials, 2019, 371, 440-448.	€% <u>C</u> O2	12
106	Mineral-derived catalysts optimized for selective catalytic reduction of NOx with NH3. Journal of Cleaner Production, 2021, 289, 125756.	4.6	12
107	Sandwich Ni-phyllosilicate@doped-ceria for moderate-temperature chemical looping dry reforming of methane. Fuel Processing Technology, 2022, 232, 107268.	3.7	12
108	Oxygen release–absorption properties and structural stability of Ce0.8Fe0.2O2â^'x. Journal of Materials Science, 2013, 48, 5733-5743.	1.7	11

#	Article	IF	CITATIONS
109	Syngas Generation from Methane Using a Chemical-Looping Concept: A Review of Oxygen Carriers. Journal of Chemistry, 2013, 2013, 1-8.	0.9	11
110	Controlled synthesis of \hat{I}_{\pm} -Fe2O3 hollows from \hat{I}^2 -FeOOH rods. Chemical Physics Letters, 2019, 731, 136623.	1.2	11
111	Layered Mg-Al spinel supported Ce-Fe-Zr-O oxygen carriers for chemical looping reforming. Chinese Journal of Chemical Engineering, 2020, 28, 2668-2676.	1.7	11
112	Electrochemical fixation of CO ₂ over a Mo plate to prepare a Mo ₂ C film for electrocatalytic hydrogen evolution. Materials Chemistry Frontiers, 2021, 5, 4963-4969.	3.2	11
113	Synthesis gas generation by chemical-looping selective oxidation ofÂmethane using Pr 1â^'x Zr x O 2â^'î oxygen carriers. Journal of the Energy Institute, 2016, 89, 745-754.	2.7	10
114	Water splitting for hydrogen generation over lanthanum-calcium-iron perovskite-type membrane driven by reducing atmosphere. International Journal of Hydrogen Energy, 2017, 42, 19776-19787.	3.8	10
115	Effect of Fe doping concentration on photocatalytic performance of CeO2 from DFT insight into analysis. AIP Advances, 2019, 9, .	0.6	10
116	Enhanced performance of the CeO2MgO oxygen carrier by NiO for chemical looping CO2 splitting. Fuel Processing Technology, 2022, 225, 107045.	3.7	10
117	Highly effective remediation of high-arsenic wastewater using red mud through formation of AlAsO4@silicate precipitate. Environmental Pollution, 2021, 287, 117484.	3.7	9
118	Promotional effect of Sn additive on the chlorine resistance over SnMnOx/LDO catalysts for synergistic removal of NOx and <i>o</i> -DCB. Catalysis Science and Technology, 2022, 12, 3863-3873.	2.1	9
119	Thermodynamic evolution of magnetite oxygen carrier via chemical looping reforming of methane. Journal of Natural Gas Science and Engineering, 2021, 85, 103704.	2.1	8
120	Enhanced Resistance to Carbon Deposition over La <i>_x</i> Ce _{1–<i>x</i>} Fe <i>_x</i> Ni _{1–<i>x</i>} O _{ Oxygen Carrier for Chemical Looping Reforming. Energy & Fuels, 2021, 35, 15867-15878.}	3<⁄2588b>	7
121	Ultrahigh photo-stable all-inorganic perovskite nanocrystals and their robust random lasing. Nanoscale Advances, 2020, 2, 888-895.	2.2	6
122	Anomalous transport controlled via potential fluctuations. Physica A: Statistical Mechanics and Its Applications, 2013, 392, 2623-2630.	1.2	5
123	Transport properties of active Brownian particles in a modified energy-depot model driven by correlated noises. Physica A: Statistical Mechanics and Its Applications, 2018, 505, 716-728.	1.2	5
124	Effect of Preparation Method on the Structural Characteristics of NiO-ZrO2 Oxygen Carriers for Chemical-looping Combustion. Chemical Research in Chinese Universities, 2019, 35, 1024-1031.	1.3	5
125	Enhancement of Reducibility and Oxygen Storage Capacity (OSC) of Ce–Fe Mixed Oxides by Repetitive Redox Treatment. Chemistry Letters, 2012, 41, 837-838.	0.7	2
126	Thermodynamics on sulfur migration in CaSO4 oxygen carrier reduction by CO. Chemical Research in Chinese Universities, 2017, 33, 979-985.	1.3	2

#	Article	IF	CITATIONS
127	Hydrostatic pressures effect on structure stability, electronic, optical and elastic properties of rutile VO ₂ doped TiO ₂ by density functional theory investigation. Materials Research Express, 2019, 6, 0965c2.	0.8	1
128	C213 TWO-STEP STEAM REFORMING OF METHANE FOR HYDROGEN PRODUCTION : THERMODYNAMIC ANALYSIS AND REACTION SYSTEM SELECTION(Hydrogen and Reforming-1). The Proceedings of the International Conference on Power Engineering (ICOPE), 2009, 2009.2, _2-2492-254	0.0	0
129	ICOPE-15-C141 CO formation by carbon oxidation over reduced CeO_2-Fe_2O_3 catalysts. The Proceedings of the International Conference on Power Engineering (ICOPE), 2015, 2015.12, _ICOPE-15ICOPE-15	0.0	Ο